Structural Engineering and Mechanics, Vol. 6, No. 3 (1998) 259-274
DOI: http://dx.doi.org/10.12989/sem.1998.6.3.259

Finite element modeling of a deteriorated R.C. slab bridge: lessons learned and recommendations

I-Kang Ho†

CICI Corporation, Taipei, Taiwan, R.O.C.

Bahram M. Shahrooz‡

Department of Civil & Environmental Engineering, University of Cincinnati, P.O. Box 210071, Cincinnati, OH 45221-0071, U.S.A.

Abstract. The test results from non-destructive and destructive field testing of a three-span deteriorated reinforced concrete slab bridge are used as a vehicle to examine the reliability of available tools for finite-element analysis of in-situ structures. Issues related to geometric modeling of members and connections, material models, and failure criteria are discussed. The results indicate that current material models and failure criteria are adequate, although lack of inelastic out-of-plane shear response in most nonlinear shell elements is a major shortcoming that needs to be resolved. With proper geometric modeling, it is possible to adequately correlate the measured global, regional, and local responses at all limit states. However, modeling of less understood mechanisms, such as slab-abutment connections, may need to be finalized through a system identification technique. In absence of the experimental data necessary for this purpose, upper and lower bounds of only global responses can be computed reliably. The studies reaffirm that success of finite-element models has to be assessed collectively with reference to all responses and not just a few global measurements.

Key words: abutment; actual structures; analytical modeling; bridge; correlation study; destructive testing; deteriorated bridges; field testing; finite element analysis; geometric modeling; linear analysis; non-destructuctive testing; nonlinear analysis; piper cap; reinforced concrete slab bridge; slab-abutment connection; slab-pier cap connection; system identification; truck load testing.

1. Introduction

Linear and nonlinear finite element analysis of structures involves geometric modeling of members and connections, simulation of damage and deterioration (if present), and selection of appropriate constitutive relationships and failure criteria. In the past two decades, studies of these issues have led to new developments such as layering concept, new failure criteria, rotating crack model, new computational tools and algorithms, etc. Most of these concepts have been verified and calibrated based on experimental data from individual elements or simple structural subassemblages. Full-scale field tests of in-situ structures into nonlinear range of behavior

† Project Design Manager
‡ Associate Professor

are rare, especially when the measured data are used for gaining further insight into modeling (e. g., Milford and Schnobrich 1984, Cluass 1989, van Mier 1987).

As part of a coordinated experimental and analytical research on performance and load-carrying capacity of constructed facilities, a 38-year old reinforced concrete slab bridge was tested nondestructively and destructively in the field (Aktan, *et al.* 1992, Miller, *et al.* 1994). In an earlier work reported by the authors and others (Shahrooz, *et al.* 1994), preliminary models were developed in an attempt to correlate the load-slab deflection curve at one location. Although the correlation efforts were inconclusive, a number of critical parameters and modeling issues were identified that would influence nonlinear response of reinforced concrete slab bridges. In the present paper, the shortcomings of the earlier study are remedied. A system identification technique in conjunction with the available global, regional, and local experimental data is utilized to develop and calibrate analytical models for connections and less understood mechanisms. The reliability of existing finite element tools for analysis of in-situ structures in the linear and nonlinear range is explored. Based on modeling insights gained from the reported analyses, recommendations for predictive analyses of similar bridges are made.

2. Description of test bridge and experimental program

2.1. Bridge geometry

The test bridge was a 38-year old, three-span, reinforced concrete, skewed slab bridge (Fig. 1). The connection between the slab and abutments consisted of standard shear keys. The slab and pier caps were of monolithic construction, with shear keys between pier caps and piers. The long-

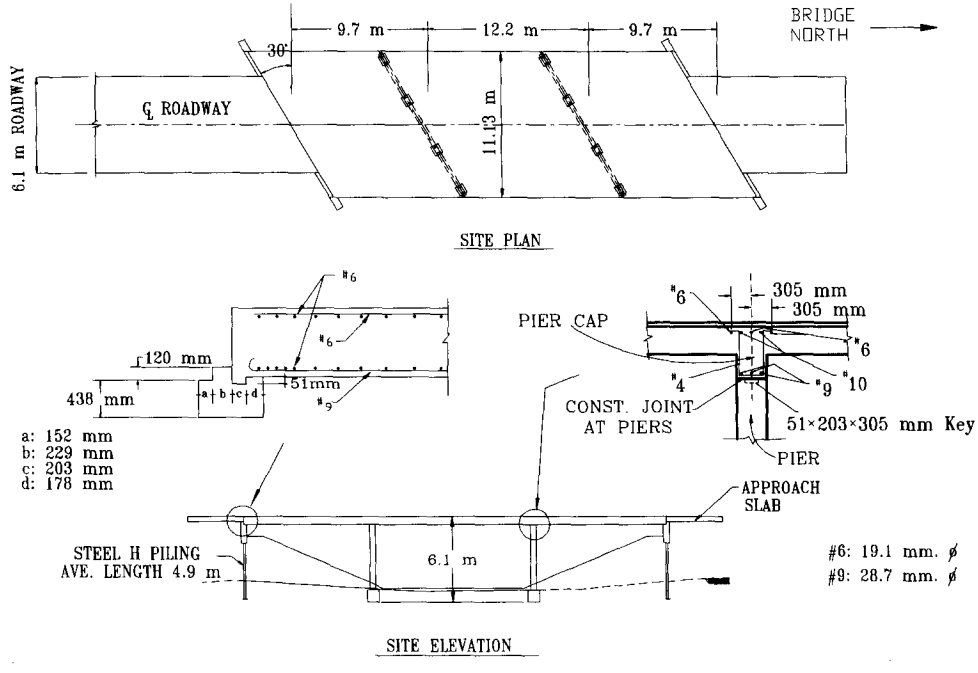

Fig. 1 Test bridge and connection details.

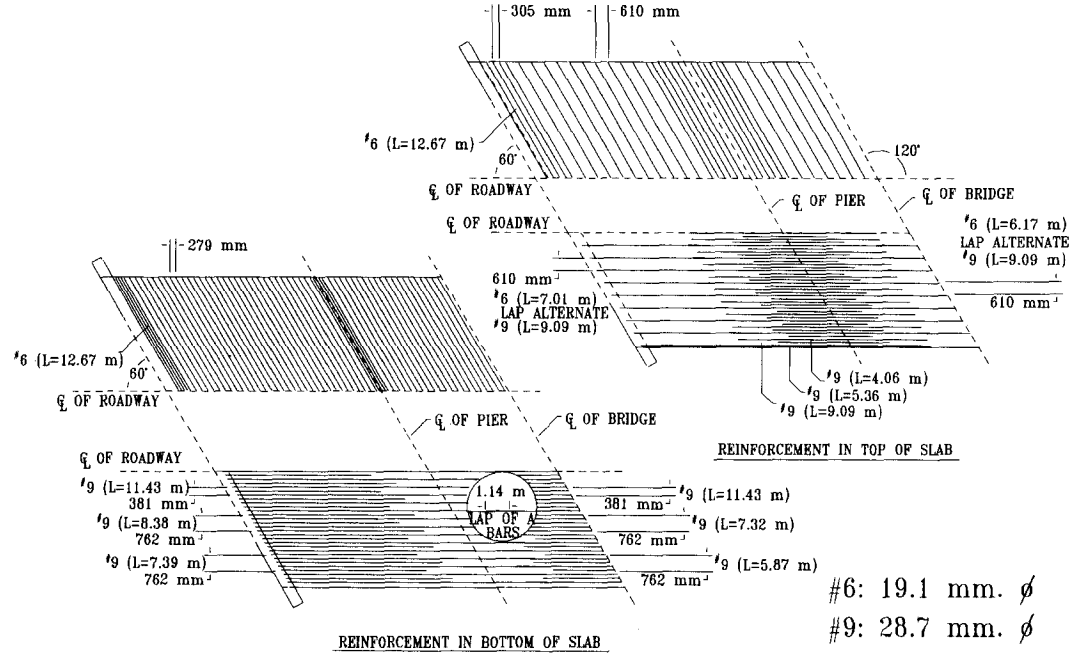

Fig. 2 Slab reinforcement.

itudinal bars in the piers extended through the shear key into the pier caps. The piers were set on footings cast on the bedrock. The two-way reinforcing bars were located within top and bottom of the slab and parallel with the slab edges. The reinforcement layout is illustrated in Fig. 2.

In general, the condition survey indicated no severe damage on the bottom side of the slab with the exception of small cracks and minor spalling. The roadway (6,000 mm wide at the center) was still in good condition, but major damage was concentrated on the top of the slab along the two shoulders over 1,830 mm to 2,440 mm wide regions. The slab reinforcing bars had lost small cross-sectional area due to corrosion; several of the top slab reinforcing bars were exposed, often debonded over a large portion of their lengths; up to 76 mm. of the concrete had spalled or deteriorated; and the quality of the concrete was considerably poorer than that in the roadway. Visual inspections and non-destructive modal tests indicated that the east shoulder was generally in a much worse condition than the west shoulder.

2.2. Material properties

Based on standard tests conducted on cores taken from the bridge deck, and No. 9 (diameter= 28.7 mm.) and No. 6 (diameter=19.1 mm.) reinforcing bar samples, the basic material properties were determined. Note that attempts to core the shoulders failed due to the very poor quality of the concrete, and the concrete properties were measured based on cores obtained from the roadway. The average values of the measured properties are summarized in Table 1.

2.3. Experimental program

The experimental phase of the research consisted of nondestructive (including modal and

Table 1 Average measured material properties

Material	Modulus of elasticity (MPa)	Compressive strength (MPa)	Yield stress (MPa)	Ultimate stress (MPa)
Concrete	34,000	51.7	–	–
No. 6 bars	199,800	–	358	725
No. 9 bars	199,800	–	345	680

truck load tests) and destructive testing (Aktan, *et al.* 1992, Miller, *et al.* 1994). The truck load tests were conducted by placing up to three single axle dump trucks (each weighing 142kN) in six different positions, and measuring the vertical deflections of the south end of the bridge deck along longitudinal and transverse grid lines parallel to the edges.

The bridge was tested to failure by loading the south span. The loads from four hydraulic actuators (which were reacting against rock anchors) were transferred to the bridge deck by means of two concrete blocks designed to produce a uniform pressure on the deck. The loads were applied at equal increments of 142kN (71kN on each block). After a series of low level tests (the total applied load during these tests was 142kN), the destructive tests were completed within two days. In the first day, the bridge was loaded up to 2,848kN, and then unloaded. The next day, the bridge was loaded to 3,130kN beyond which the bridge failed in a brittle manner. The final failure appeared to have begun as a shear failure in the shoulder region. The failure in the deteriorated area then propagated into the sound areas of the slab as a dynamic front. The slab reinforcing bars had just yielded at a few locations when the bridge failed. The flexural capacity of the slab had not been developed at failure.

3. Correlation studies and modeling issues

A system identification approach was followed to develop an analytical model that could successfully replicate the measured responses. As a first step, linear finite element analyses were used to construct geometric models of slab-pier cap-pier connection and slab-abutment connection; and to find a simple method for incorporating the damage along the shoulders. These analyses formed the basis for constructing the nonlinear finite element models.

4. Linear finite element analyses

4.1. Overall geometric model

The bridge was modeled by SAP90 (Habibullah and Wilson 1989) as shown in Fig. 3. An isotropic shell element, which includes plate bending and membrane actions, was used to model the bridge deck. Variation of Poisson's ratio between 0.15 and 0.2 did not significantly affect the computed results (Ho and Shahrooz 1993), and it was taken as 0.2. The average measured concrete modulus of elasticity was used in the analyses.

4.2. Simulation of damage

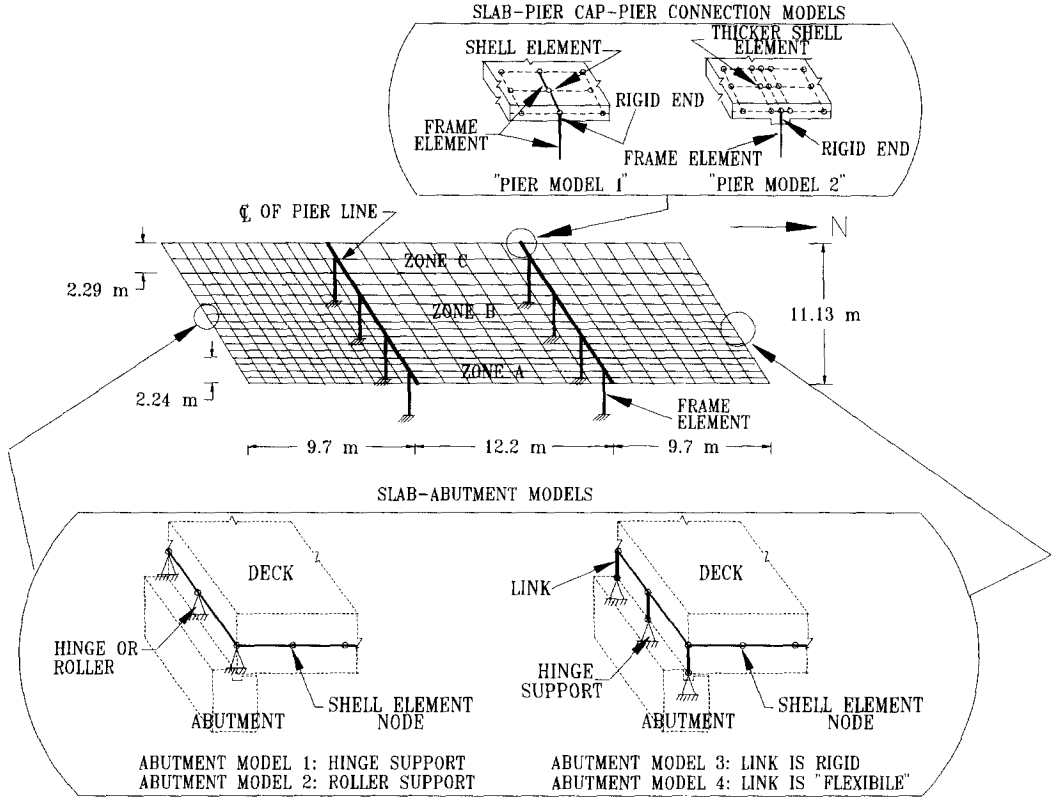

Fig. 3 Linear finite element model.

The potential slippage of top reinforcing bars in the deteriorated slab in conjunction with poor quality concrete would reduce the slab stiffness in the shoulder regions. Detailed experimental data about bond-slip characteristics of the reinforcing bars and local variation of concrete properties in the damaged shoulders were not available. In order to avoid a trial and error method for assigning different stiffnesses to the damaged and undamaged portions of the bridge deck, the damage was approximately simulated by reducing the slab thickness in the shoulders according to available field measurements. The slab thickness along the eastern (zone A in Fig. 3) and western (zone C in Fig. 3) shoulders was reduced by 76 mm. and 25 mm., respectively. The nominal thickness of 438 mm. was used for the driving lanes (zone B in Fig. 3).

4.3. Modeling of slab-pier cap-pier connection

A number of methods may be followed to model the slab-pier cap-pier connection. Two models are considered herein, and are referred to as "pier model 1" and "pier model 2" - refer to Fig. 3. In both models, the piers are modeled by frame elements. A rigid end zone equal to the pier cap thickness plus half slab thickness is specified at the top of each of these frame elements. In pier model 1, a horizontal frame element is used to represent each pier cap, and it is connected to the shell elements which model the bridge deck. The properties of this frame element are computed according to the cross-sectional dimensions of the pier cap. In pier model 2, the horizontal frame element (used to model pier cap in pier model 1) is replaced by a thicker

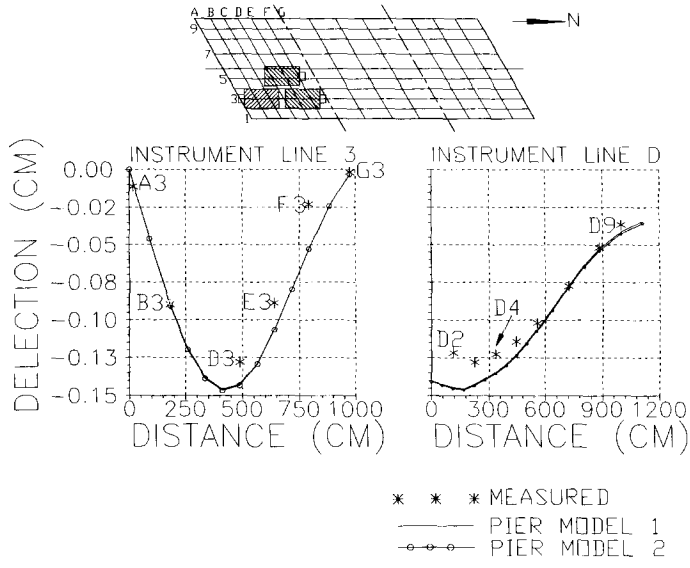

Fig. 4 Effects of slab-pier cap modeling on deflection profiles for three-truck load test.

shell element, as shown in Fig. 3. The width and thickness of the thicker shell elements coincide with the corresponding pier cap dimensions.

Using these two models, the deflection profiles for various truck load tests were computed and compared to the measured data. In all the analyses, the damage on the shoulders was incorporated as discussed previously, and the slab-abutment connections were modeled by attaching shell elements nodes directly to hinge supports, i.e., abutment model 1 shown in Fig. 3. A more detailed discussion regarding modeling of slab-abutment connection will be provided in the next section. The results along instrument line 3 and line D for a case with three trucks are summarized in Fig. 4. This particular configuration of the trucks is used for illustration herein as it produces the largest deflections. The deflection profiles are clearly not affected by how the slab-pier cap-pier connection is modeled. Hence, in all the subsequent analyses pier model 1 is used because it is simple yet it does not adversely affect the response. This observation is also valid for nonlinear finite element analyses because the experimental data from the destructive test do not suggest inelastic action in the piers and pier caps. The observed poor correlation of the experimental deflection profiles is attributed to problems associated with modeling of the slab-abutment connection, as discussed next.

4.4. Modeling of slab-abutment connection

Slab-abutment connections are commonly modeled by attaching shell elements nodes, which are located at the bridge deck mid-depth, directly to hinge or roller supports. This model fails to recognize that shear keys at slab-abutment connection are located at the bottom of the slab and not at its mid-depth. Even if the bridge deck is restrained horizontally by the shear keys at the abutment level, the rotation of the bridge deck would result in an apparent horizontal movement at the mid-depth of the slab where the shell elements are located. This mechanism is illustrated in Fig. 5, and needs to be modeled.

Four slab-abutment connection models were considered (Fig. 3). In abutment model 1 and

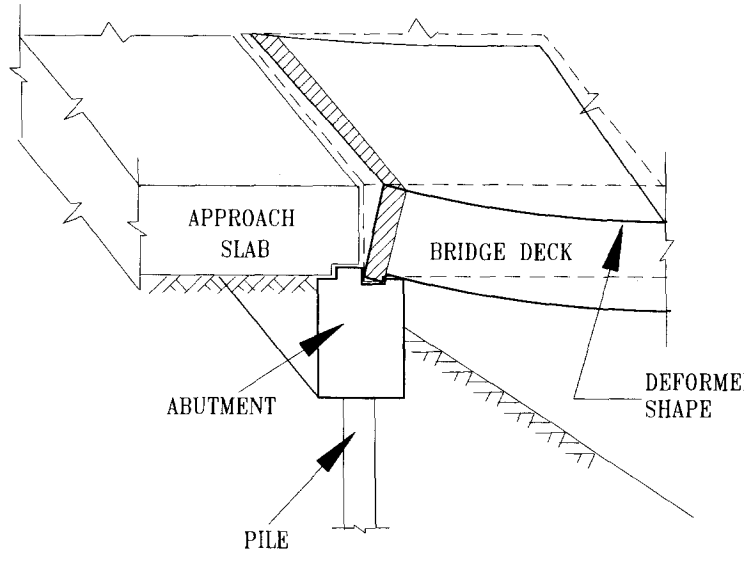

Fig. 5 Slab rotation at abutment.

model 2, the shell elements are supported by hinges or rollers, respectively. In an attempt to reproduce the expected behavior shown in Fig. 5, two other models were considered. Abutment model 3 consists of rigid links that connect the shell elements to hinges located at elevations corresponding to the shear keys. Abutment model 4 is similar to abutment model 3 except that the rigid links are replaced by frame elements with cross-sectional properties equal to those from a portion of the slab above the shear key (i.e., the cross hatched region in Fig. 5). In all the analyses, the damage along the two shoulders was modeled as discussed before, and pier model 1 was used to represent the slab-pier cap-pier connection.

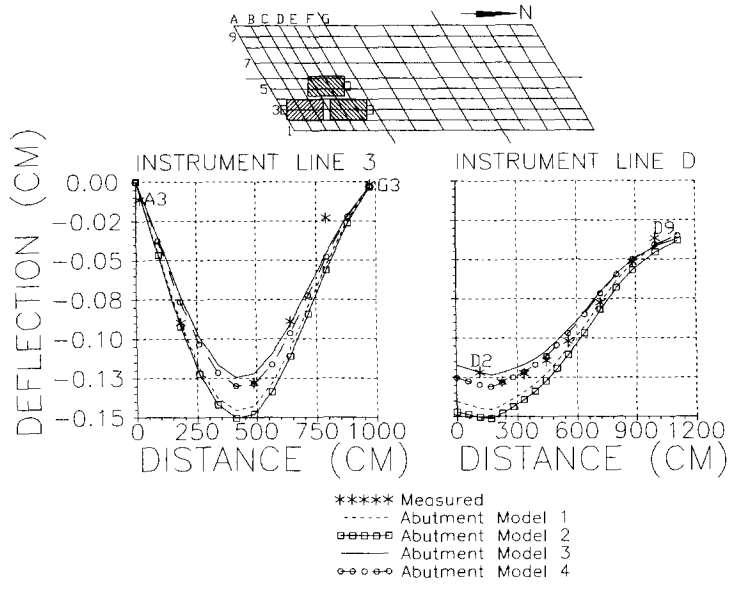

Fig. 6 Effects of pier-abutment modeling on deflection profiles for three-truck load test.

Fig. 6 indicates that abutment model 1 and model 2 overestimate the measured deflections, but the two results are not significantly different. The computed deflections from abutment model 3 and model 4 are also close. The analytical deflection profiles from these two models follow the experimental data more reasonably. Based on the results shown in Fig. 6 and those for other load cases and instrument lines reported elsewhere (Ho and Shahrooz 1993), abutment model 4 appears to most reliably simulate the stiffness of the slab-abutment connection under service loads. A plausible enhancement to abutment model 4 is to introduce rotational springs at the hinges. Nevertheless, parametric studies conducted by Ho and Shahrooz (1993) do not suggest that the computed responses are affected by lack or presence of such springs.

5. Nonlinear finite element analyses

5.1. Geometric characteristics of model

The computer program POLO-FINITE (Lopez, *et al.* 1987) was used to conduct the nonlinear finite element analyses. The bridge deck was modeled by a 9-node degenerate isoparametric shell element with a nonlinear material model (Milford and Schnobrich 1984). An overall view of the model is shown in Fig. 7. According to the observations made from the linear analyses, the damage along the two shoulders was incorporated by reducing the slab thickness. The slab-pier cap-pier connections were modeled according to pier model 1. Frame elements with elastic material model were used to represent the piers. As described later, two models were used to simulate the slab-abutment connections.

5.2. Slab reinforcement and steel material properties

The stress-strain curve for the reinforcing steel in tension and compression was idealized as elastic-strain hardening, with the critical values set equal to the average measured values. A smeared model was used to represent the slab reinforcing bars which were quantified by the direction of bars and reinforcement ratio at each Gauss point of the shell elements. The slab reinforcement in the damaged and undamaged regions were assumed to have perfect bond. Although this assumption is reasonable for the bars located in the driving lanes, the shoulder reinforcing bars are expected to exhibit local slip. The necessary experimental data were not available to simulate the bond slip in the analyses. Dowel action of the reinforcing bars across cracks was not modeled.

5.3. Concrete material properties

The nonlinear compressive behavior of the concrete stress-strain relationship was incorporated by using a model proposed by Milford and Schnobrich (1984), as shown in Fig. 7. The values shown in this figure are based on the average measured properties. A bilinear function similar to that suggested by Gilbert and Warner (1978) was used to assess post-cracking behavior. Other available models (e.g., Vecchio-Collins 1986, Okamura, *et al.* 1985) exhibit residual tensile strength at very large concrete tensile strains. Such residual stresses are not reasonable for a reinforced concrete slab with little or no confinement particularly if it is deteriorated. In the bilinear function, the strain at which the tensile stress drops to zero was taken as 10 times the cracking

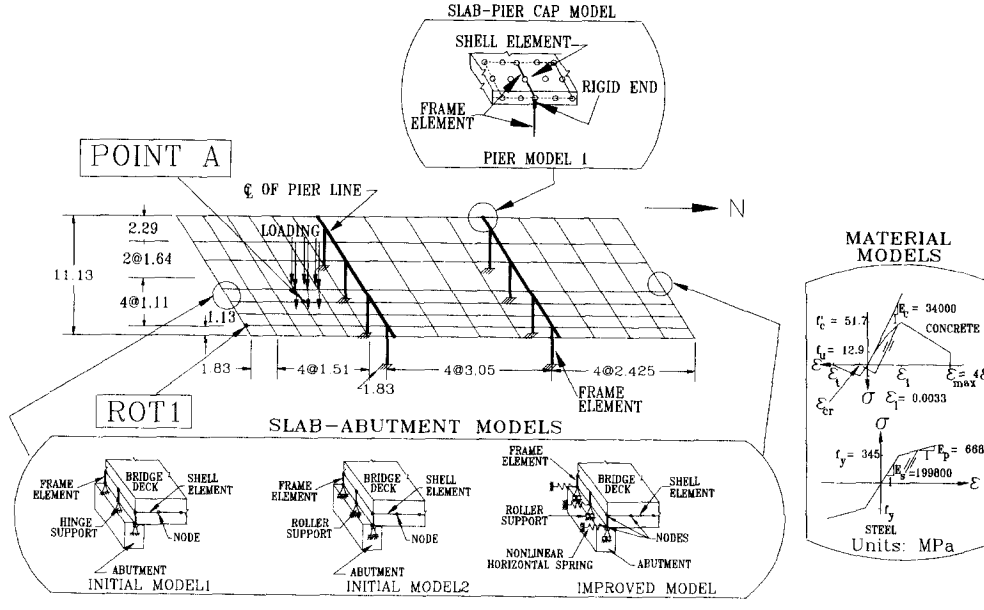

Fig. 7 Nonlinear finite element model.

strain. Consistent with previous studies (Massicotte, *et al.* 1990, Mau and Hsu 1987, Gilbert and Warner 1978, and Chen 1982) the concrete tensile strength was assumed to range from $0.33\sqrt{f'_c}$ (2.41 MPa) to $0.41\sqrt{f'_c}$ (2.98 MPa), where f'_c is the concrete compressive strength expressed in MPa. A rotating crack model (Gupta and Habibullah 1982) was used in which the directions of cracks always remain normal to the direction of the principal strain.

Shear transfer in concrete across cracks may be simulated by reducing the value of shear modulus after formation of cracks. This can be accomplished by a reduction factor commonly referred to as shear retention factor which reasonably ranges between 0.1 and 0.5 (e.g., Barzegar 1989). Parametric nonlinear analyses (Ho and Shahrooz 1993) did not show any appreciable change in the global responses if the shear retention factor is taken as 0.25 or 0.4. In all the analyses, this factor was set to 0.25.

A four-parameter failure criterion defined by a triaxial stress function (Hsieh, *et al.* 1982) was used. This function is

$$F(I_1, J_2, \sigma_1) = A\frac{J_2}{f'_c} + B\sqrt{J_2} + C\sigma_1 + DI_1 - f'_c = 0$$

where f'_c=concrete compressive strength, σ_1=the principal stress, I_1=the first stress invariant, and J_2=the second deviatoric stress invariant. By curve fitting to the experimental data by Kupfer and Gerstle (1973), Gallegos-Cazares and Schnobrich (1988) found the values of A, B, C, and D to be 2.0108, 0.9714, 9.1412, and 0.2312, respectively.

5.4. Initial model 1

Abutment model 4 (see Fig. 3) was used as a reasonable initial attempt to simulate the slab-abutment connections. Modeling of slab, piers, and slab-pier cap-pier connection; and material

constitutive relationships are as discussed previously.

The load-deflection at point A (refer to Fig. 7 for its location) is compared with the experimental data in Fig. 8. The value of concrete tensile strength does not significantly influence the computed responses. A higher concrete tensile strength ($0.41\sqrt{f'_c}$=2.98 MPa) expectedly produces a slightly stiffer response. Taking the concrete tensile strength as $0.33\sqrt{f'_c}$ (2.41 MPa), a rather good correlation of the experimental strength and stiffness is possible for loads as large as 2280 kN which corresponds to 73% of the ultimate measured load. Beyond this point, the computed load-deflection deviates from the experimental data. The deflection profiles along instrument lines D and 4 shown in Fig. 9(a) confirm this observation. Based on these global measurements, one might be led to believe that the model successfully captures the response of the bridge up to a total load of 2280 kN. However, a regional measurement such as slab rotation along the south abutment indicates otherwise. As seen from Fig. 10, not only does the computed slab rotation at ROT1 (the location is shown in Fig. 7) fail to match the measured rotation, but it decreases beyond about 1780 kN while the experimental data show a continuously increasing trend with larger loads. This observation points to the futility of assessing the success of a finite element model by considering only a few global responses.

5.5. Improved model

Assuming that the shear keys between the abutments and bridge provide sufficient restraint against horizontal movement, the slab-abutment connection in the initial model was represented by hinge supports located at the shear key elevations. The horizontal reaction force at the shear key, particularly at large loads, may exceed the available frictional resistance which in turn can cause the slab to move horizontally (Zwick, *et al.* 1992, Miller, *et al.* 1994). In an idealized case where the shear key is undamaged and/or the slab corners near the shear key are perfectly square, the horizontal movement is limited to the available gap between the two components. Despite obvious difficulties for establishing the level of horizontal movement in actual structures, the geometric model should allow for such a movement so that the membrane force in the slab is "regulated". This regulation will become particularly critical in advanced nonlinear range when the slab deformations could lead into large membrane forces if the slab is restrained horizontally.

The initial model was revised by using nonlinear horizontal springs which were attached to rollers at elevations corresponding to the shear keys. The improved slab-abutment model is illustrated in Fig. 7. Based on the observations made for initial model 1, the concrete tensile strength was taken as $0.33\sqrt{f'_c}$=2.41 MPa. Due to insufficient experimental data measuring the movement of the slab at the abutment, a system identification procedure had to be followed to characterize the springs. Each spring was assumed to have a trilinear load-deflection response as shown in Fig. 11(a). The loss of stiffness after the first break point is intended to simulate loss of frictional resistance, i.e., prior to the first break point the springs should act as hinges. Parametric studies by Ho and Shahrooz (1993) indicate that so long as the initial stiffness (K_1) is large to simulate a hinge, the computed responses are not affected by the exact value of K_1. The initial model could reasonably correlate the measured load-deflection, deflection profiles, and most importantly slab rotation up to a total load of 540 kN (see Figs. 8, 9, 10). Hence, the initial stiffness was fine tuned so that when the total load on the bridge is 540 kN, the computed displacement in each spring would be approximately 0.12 mm. Other large values of K_1

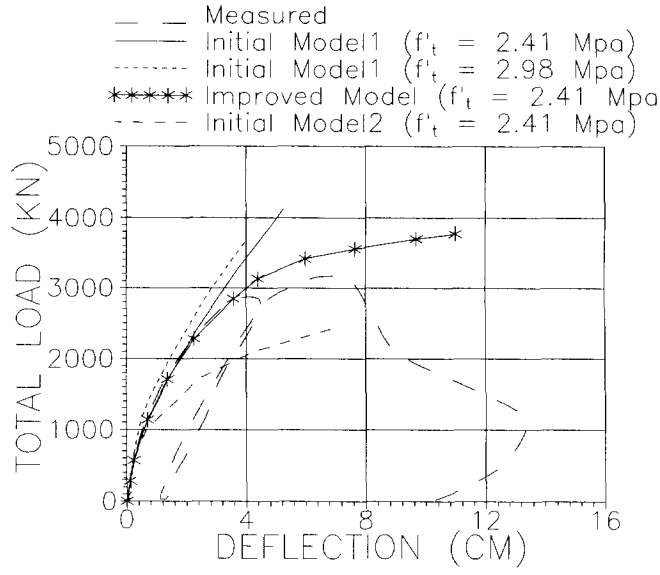

Fig. 8 Load-deflection relationship.

did not change the results (Ho and Shahrooz 1993). The stiffness after the second break point is automatically set to zero by the finite-element code. Hence, only the slope of the second segment and the loads or deflections at the two break points need to be calibrated as described in the following.

5.5.1. Location of break point No. 1

An analysis was performed by assigning a large value of deflection at the first break point of each horizontal spring, i.e., 25 mm. By comparing the computed load-deflection, displacement profiles, and slab rotation with the experimental data at each load increment, the maximum total up to which a good correlation was still possible could be established. The load in each horizontal spring corresponding to this load step was, then, used to determine the deflection at the first break point for each spring. The procedure is shown schematically in Fig. 11(b).

5.5.2. Slope of segment No. 2

By giving different values to the second slope (K_2), the deflection profiles were computed. This procedure was repeated until an optimal slope leading to a good correlation was possible.

5.5.3. Location of break point No. 2

In order to avoid numerical instability, the load at the second break point (load P_2 in Fig. 11(a)) was defined to be larger than the load in that spring when the ultimate load is developed. In this manner, the load in each spring would never exceed load P_2.

Based on the aforementioned procedure, four groups of springs were identified - type A, B, C, and D shown in Fig. 11(c). The springs were grouped based on mesh size and whether a spring would be at a middle or a corner node. Springs coinciding with middle nodes would clearly

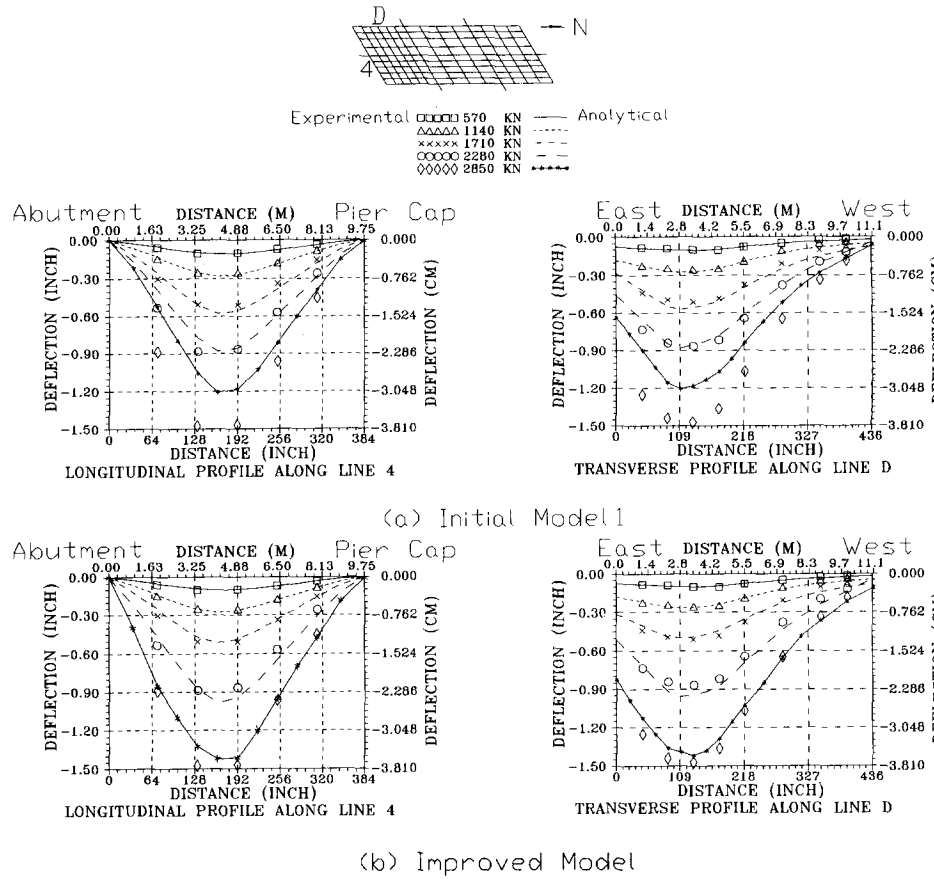

Fig. 9 Deflection profiles at different levels of loading.

have a larger stiffness. The initial stiffness (K_1) of the springs at the middle nodes (spring type B) was found to be approximately 1.61 times larger than the corresponding value for the springs at the corner nodes (type C). This ratio is rather close to the value obtained based on "work-equivalent load". It is emphasized that the identified springs are not unique and other equally acceptable values are possible.

5.6. Results from improved model

5.6.1. Global response

The computed load-deflection curve (Fig. 8) compares rather well with the experimental results up to 2848 kN. After this load, the analytical model shows a slightly stiffer response which is attributed to the influence of large out-of-plane shearing stresses which are not incorporated in the failure criteria. The deflection profiles along two representative longitudinal and transverse instrument lines are also closely matched, refer to Fig. 9(b).

5.6.2. Regional response

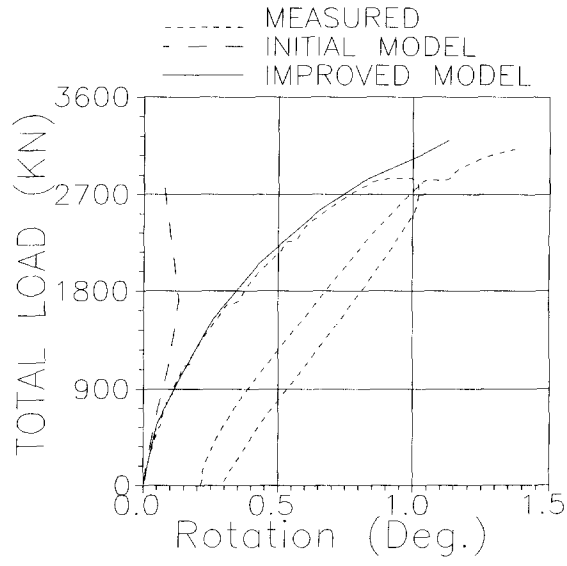

Fig. 10 Load-slab rotation relationship.

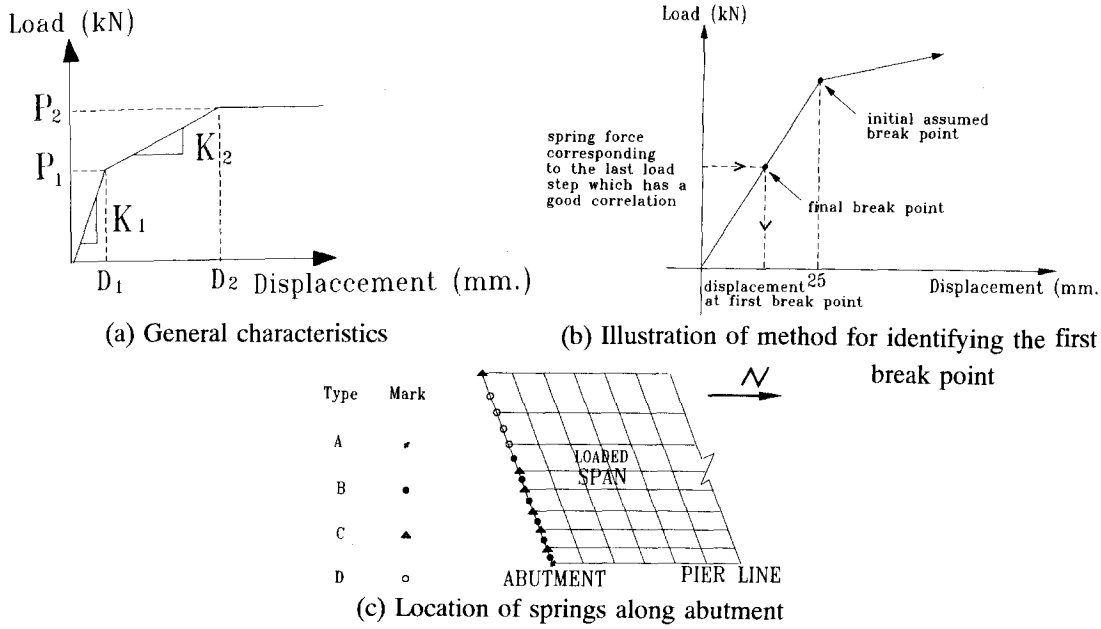

(a) General characteristics

(b) Illustration of method for identifying the first break point

(c) Location of springs along abutment

Fig. 11 Nonlinear horizontal spring at abutments

The analytical and experimental load-slab rotation curves at location ROT1 (see Fig. 7 for the location) are compared in Fig. 10. A very good correlation is evident.

5.6.3. Local response

The computed locations of the first yielding of the slab reinforcing bars are shown in Fig. 12. The total load at initiation of the first yielding is 2848 kN which is very close to the measured

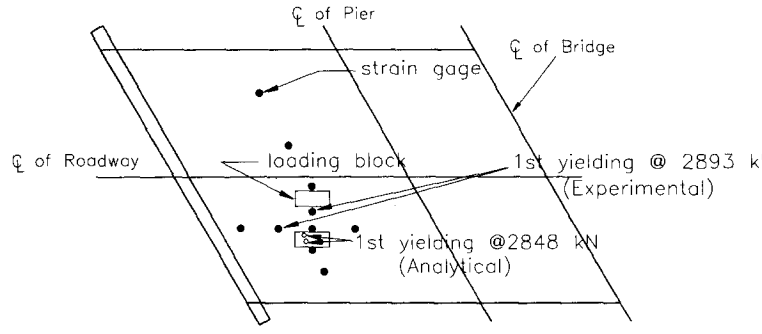

(a) Longitudinal Reinforcement

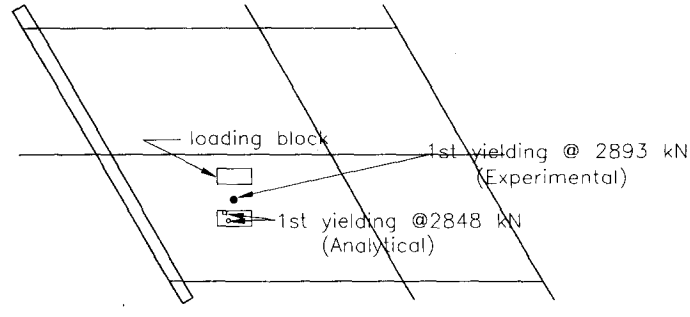

(b) Transverse Reinforcement

Fig. 12 Location of computed and measured initial yielding in slab reinforcement.

value of 2890 kN. The locations of the yielded bars are matched very reasonably as well.

5.7. Epilogue

The preceding discussion points to the importance of proper simulation of the stiffness of slab-abutment connection which had to be calibrated based on experimental data. Such data are not typically available. In such cases, only the upper and lower bounds of global responses can reasonably be computed. The stiffness of the trilinear springs in the improved model is between zero and that of a fully-restrained support. These bounds may be simulated by rollers (i.e., initial model 2 shown in Fig. 7) and hinges (i.e., initial model 1), respectively. As illustrated in Fig. 8, the measured load-deflection is bound by the results from these slab-abutment connection models. Previous discussion of initial model 1 shows that such models are not expected to match regional and local responses. However, these models can provide an insight into load-carrying capacity and stiffness which are typically the primary indices for bridge engineers.

6. Summary, conclusions, and recommendatios

A number of issues related to finite-element modeling of actual structures were examined with reference to the experimental data from non-destructive and destructive field testing of a three-span deteriorated reinforced concrete slab bridge. Based on the reported analyses, the following

observations are made.

(1) Data necessary to simulate damage at a macroscopic level are not typically available. The loss of slab stiffness due to damage may be approximately taken into account by reducing the thickness in the damaged regions according to field measurements.

(2) Geometric modeling of slab-pier cap-pier connection did not appreciably affect the response. This connection can be simulated by a number of reasonable models, such as pier model 1 shown in Fig. 3.

(3) The common procedure of attaching shell elements nodes to hinges or rollers at abutments fails to capture the expected behavior at slab-abutment connections. For linear analyses, abutment model 4 illustrated in Fig. 3 is recommended. For the test bridge, this model could also replicate the global, regional, and local responses in the nonlinear range up to a total load equivalent to 4 rating trucks. However, this model fails to simulate slip of the slab at the shear key, and the correlation of the measured data (particularly of the regional and local responses) becomes unacceptable at higher loads. In order to "regulate" the slab membrane force in advanced nonlinear range, the hinge supports in abutment model 4 were replaced by nonlinear horizontal springs with trilinear load-deflection characteristics. The information needed to define the springs was identified through the available experimental data. Using the revised slab-abutment connection model, it was possible to correlate the measured global, regional, and local responses at all limit states.

The experimental data used to calibrate the horizontal springs are not typically available. In such cases, nonlinear analyses can be expected to only establish reasonable upper and lower bounds of capacity and stiffness which are of primary importance to bridge engineers. Abutment model 4 is recommended to compute the upper-bound values. The lower-bound values can be determined by using rollers instead of hinges in abutment model 4. However, such models are not expected to reliably predict regional and local responses.

(4) The correlation studies clearly indicate that the success of a finite element model has to be gauged collectively with reference to data at all levels rather than just a limited number of global responses.

(5) Available material constitutive models and failure criteria are apparently adequate. Local variables such as Poisson's ratio or shear retention factor do not influence the response significantly, and values within accepted limits can be used. Special attention must be paid to concrete tensile strength and post-cracking behavior. A lower bound value of concrete tensile strength, and a bilinear concrete post-cracking model are recommended for reinforced concrete slab bridges. The strain at which the tensile stress drops to zero should be between approximately 7 to 12 times the cracking strain. Lack of inelastic out-of-plane shear response in most nonlinear shell elements is a major shortcoming that needs to be overcome.

Acknowledgements

The research presented herein is based on an investigation supported by the National Science Foundation under Grant No. MSM-9002820, with Dr. Ken P. Chong as the program director, and by the Federal Highway Administration and Ohio Department of Transportation Contract No. 14482. Any opinions, findings, and conclusions or recommendations expressed in this paper are of those of the authors and do not necessarily reflect the views of the sponsors. Professors Lopez and Schnobrich from the University of Illinois at Urbana-Champaign provided POLO-FINITE program, and were always helpful. Their assistance is gratefully thanked.

References

Aktan, A.E., Zwick, M., Miller, R.A. and Shahrooz, B.M. (1992), "Nondestructive and destructive testing of a decommissioned RC slab highway bridge and associated analytical studies", *Transportation Record* No.1371, Transportation Research Board.

Barzegar, F. (1989), "Analysis of RC membrane elements with anisotropic reinforcement", *J. Struct. Engrg., ASCE,* **115**(3), 647-665.

Clauss, D.B. (1989), "Round-robin analysis of the behavior of 1:6-scale R.C. containment model pressurized to failure: post-test evaluations", *NUREG/CR*-5341-*SAND*89-0349, Sandia National Laboratories, Nuclear Regulatory Commission, Washington, D.C.

Chen, W.F. (1982), "Plasticity in reinforced concrete", McGraw-Hill, Inc.

Gallegos-Cazares, S. and Schnobrich, W.C. (1988), "Effects of creep and shrinkage on the behavior of reinforced concrete gable and roof hyperbolic-paraboloids", *Civil Engineering Series, SRS* No. 543, University of Illinois at Urbana-Champaign, Illinois.

Gilbert, R.I. and Warner, R.F. (1978), "Tension stiffening in reinforced concrete slabs", *J. Struct. Engrg., ASCE,* **104**(12), 1885-1900.

Gupta, A.K. and Habibullah, A. (1982), "Changing crack direction in reinforced concrete analysis", Report, Department of Civil Engineering, North Carolina State University, Rayleigh, North carolina, January, 1982.

Habibullah, A. and Wilson, E.L. (1989), *SAP90 User's Manual.* Computers & Structures Inc., Berkeley, CA.

Ho, I.K. and Shahrooz, B.M. (1993), "Nonlinear finite element analysis of a deteriorated reinforced concrete slab bridge", *Report No. UC-CII* 93/02, Cincinnati Infrastructure Institute.

Hsieh, S., Ting, E. and Chen, W.F. (1982), "A plastic fracture model for concrete", *International Journal of Solids and Structures,* **18**(3), 181-197.

Kupfer, H. and Gerstle, K.N. (1973), "Behavior of concrete under biaxial stress", *J. Eng. Mech. Div.., ASCE,* **99**(4), 852-866.

Lopez, L.A., Dodds, R.H., Rehak, D.R. and Schmidt, R.J. (1987), "POLO-FINITE: a structural mechanics system for linear and nonlinear, static and dynamic analysis", Civil Engineering Systems Laboratory, University of Illinois at Urbana-Champaign, Illinois; Department of Civil Engineering, University of Kansas, Lawrence, Kansas; Department of Civil Engineering, Carnegie-Mellon University, Pittsburgh, Pennsylvania, and Department of Civil Engineering, University of Wyoming, Laramie, Wyoming.

Massicotte, B., Elwi, A.E. and MacGregor, J.G. (1990), "Tension-stiffening model for planar reinforced concrete members", *J. Struct. Engrg., ASCE,* **116**(11), November, 3039-3058.

Mau, S.T. and Hsu, T.C. (1987), "Shear strength prediction for deep beams with web reinforcement", *ACI Structural Journal*, Nov.-Dec. 513-523.

Milford, R.V. and Schnobrich, W.C. (1984), "Nonlinear behavior of reinforced concrete cooling towers", *Civil Engineering Studies, Structural Research Series*, No. 514, University of Illinois at Urbana-Champaign.

Miller, R.A., Aktan, A.E. and Shahrooz, B.M. (1994), "Destructive testing of a decommissioned concrete slab bridge", *J. Struct. Engrg., ASCE,* **120**(7), 2176-2198.

Okamura, H., Maekawa, K. and Sivasubramaniyam, S. (1985), "Verification of modeling for reinforced concrete finite element", *In Finite Element Analysis of Reinforced Concrete Structures*, edited by Meyer Ch., and Okamura H., Published by ASCE, 528-543.

Shahrooz, B.M., Ho, I.K., Aktan, A.E., Borst, R., Blaauwendraad, J., Veen, C., Iding, R.H. and Miller, R. A. (1994), "Nonlinear finite element analysis of a deteriorated R.C. slab bridge", *J. Struct. Engrg. , ASCE,* **120**(2), 422-440.

van Mier, J.G.M. (1987), "Examples of nonlinear analysis of reinforced concrete structures with DIANA", *HERON*, **32**(3).

Vecchio, F.J. and Collins, M.P. (1986), "The modified compression-field theory for reinforced concrete elements subjected to shear", *ACI Struc. J.,* **83** (2), 219-231.

Zwick, M. *et al.* (1992), "Nondestructive and destructive testing of a RC slab bridge and associated analytical studies", *Report No.UC-CII* 92/02, University of Cincinnati.